Biomaterials 262 (2020) 120248

Contents lists available at ScienceDirect

Biomaterials

journal homepage: www.elsevier.com/locate/biomaterials

A fully defined 3D matrix for *ex vivo* expansion of human colonic organoids from biopsy tissue

Fredrik Bergenheim [a,*], Giulia Fregni [b], Cara Field Buchanan [b], Lene Buhl Riis [c], Mathieu Heulot [b], Jeremy Touati [b], Jakob Benedict Seidelin [a,1], Simone Carlo Rizzi [b,*,1], Ole Haagen Nielsen [a,1]

[a] Dept. of Gastroenterology, Herlev Hospital, University of Copenhagen, 2730 Herlev, Denmark
[b] QGel SA, Innovation Park, EPFL Building G, 1015 Lausanne, Switzerland
[c] Dept. of Pathology, Herlev Hospital, University of Copenhagen, 2730 Herlev, Denmark

ARTICLE INFO

Keywords:
Cell differentiation
Extracellular matrix
Human colonic organoids
Hydrogel
Intestinal stem cells

ABSTRACT

Intestinal organoids have widespread research and biomedical applications, such as disease modeling, drug testing and regenerative medicine. However, the transition towards clinical use has in part been hampered by the dependency on animal tumor-derived basement membrane extracts (BMEs), which are poorly defined and ill-suited for regulatory approval due to their origin and batch-to-batch variability. In order to overcome these limitations, and to enable clinical translation, we tested the use of a fully defined hydrogel matrix, QGel CN99, to establish and expand intestinal organoids directly from human colonic biopsies. We achieved efficient *de novo* establishment, expansion and organoid maintenance, while also demonstrating sustained genetic stability. Additionally, we were able to preserve stemness and differentiation capacity, with transcriptomic profiles resembling normal colonic epithelium. All data proved comparable to organoids cultured in the BME-benchmark Matrigel. The application of a fully defined hydrogel, completely bypassing the use of BMEs, will drastically improve the reproducibility and scalability of organoid studies, but also advance translational applications in personalized medicine and stem cell-based regenerative therapies.

1. Introduction

Since the pivotal discovery of effective culture protocols for intestinal organoids [1], organoid culture development has rapidly evolved, and is now being used in a vast array of different fields of life science research. The diagnostic and therapeutic uses of these techniques are receiving increasing focus [2,3], and advances in the last decade have built the foundation for organoids to be applied for personalized drug screening [4,5] and regenerative medicine [6–8], as well as a tool for studying disease mechanisms and therapeutic signaling pathways [9,10]. Despite these scientific breakthroughs and their potential for clinical applications, translation of organoid use in regenerative or personalized medicine remains challenging. This is in large part because standardization and reproducibility are hindered by the dependency on animal tumor-derived basement membrane extracts (BMEs), such as Matrigel [11], which are poorly defined (containing more than a thousand proteins and peptides, including varying amounts of sarcoma-derived growth factors) and display limited lot-to-lot similarity (approximately 53%) [12,13]. Combined, these aspects hamper regulatory approval and thereby clinical application as well [11].

To address these considerable limitations of BMEs, extensive progress has been made in developing viable alternatives, such as collagen matrices [8,14,15] as well as hydrogels based on fibrin [16], polyethylene glycol [17–19] or alginate [20]. However, published data on these alternatives contain limited information on the long-term efficiency of stem cell maintenance, quantity of cells obtained after expansion, cell differentiation capacity, and especially on *de novo* establishment of organoids (i.e., directly from human tissue without pre-amplification in BMEs). Natural materials, such as collagen are cyto-compatible but may display batch-to-batch variability, uncontrolled stiffness and limited long-term stability [21]. In turn, fully defined matrices offer the possibility to tune key characteristics, such as

* Corresponding authors.
E-mail addresses: Fredrik.Bergenheim@regionh.dk (F. Bergenheim), Simone.Rizzi@qgelbio.com (S.C. Rizzi).
[1] Shared senior authorship.

https://doi.org/10.1016/j.biomaterials.2020.120248
Received 19 December 2019; Received in revised form 15 June 2020; Accepted 16 July 2020
Available online 19 August 2020

their biological (e.g., by incorporation of cell-cell and cell-matrix binding sites), biophysical (e.g., by varying stiffness) and biochemical (e.g., by incorporation of cell-mediated degradability) properties for specific cell types and can also be produced with high quality and consistency. Yet, the previously reported manufacturing processes for functionalized hydrogels are technically demanding, thus requiring extensive experience in biomaterials and bioengineering, significantly limiting the general applicability.

Transition of the organoid culture platform and its different applications towards clinical use, requires efficient and highly reproducible protocols [22]. This thereby necessitates that the extracellular matrix (ECM) be fully defined, scalable and manufactured in compliance with clinical application-specific regulatory requirements. With these key aspects in mind, we have tested the use of QGel CN99, an easy-to-use and fully defined hydrogel-based ECM, to establish and grow human colonic organoids directly from fresh biopsy tissue, thus bypassing the use of animal-based BMEs. The organoids grown in CN99 were maintained and expanded for at least six culture passages, while sustaining both the stem cell self-renewal as well as the multilineage differentiation capacity. A schematic illustration of the study design and readouts is depicted in Fig. 1.

2. Materials and methods

2.1. Isolation of crypt-derived single cells from human colonic biopsies

Punch biopsies were obtained from the left side of the colon from healthy control subjects (n = 10) as well as from patients with quiescent ulcerative colitis (n = 2) (i.e., Mayo score of 0) [23] after informed consent. The basic clinical information of patients is summarized in Table 1. Samples were processed either freshly (ID#1–2; 6–11) or after a maximum of 24 h (ID#3–5 and 12) on ice in basal medium (advanced Dulbecco's Modified Eagle Medium/F12 (DMEM/F12, Thermo Fisher, Waltham, MA, USA), GlutaMAX (1x) (Thermo Fisher), Pen-Strep (100 U/ml) (Thermo Fisher or Bioconcept AG, Allschwil, Switzerland), HEPES (10 mM) (Thermo Fisher) and ROCK inhibitor Y-27632 (10 μM) (Sigma-Aldrich, St. Louis, MO, USA)). The biopsies were transferred to ice-cold Dulbecco's Phosphate-Buffered Saline (DPBS, Thermo Fisher) containing dithiothreitol (0,5 mM) (DTT, Bio-Rad Laboratories, Hercules, CA, USA), and were washed four times. Ethylenediaminetetraacetic acid (8 mM) (EDTA, Thermo Fisher) was added and the sample tube was placed on a tilt-table at 5 °C. After 60 min the supernatant was replaced with new DPBS and the tube was shaken to release the crypts. The

Table 1
Baseline data.

Parameter	Count	
Total number of cell donors:	12 (ID#1–12)	
Gender:	**Male**	**Female**
	8	4
Age:	Median = 54 years (ICR = 52–62 years)	
Colonic region biopsied:	Sigmoid/descending colon (n = 12)	
Intestinal status:	**No colonic disease**	**Quiescent ulcerative colitis**
	10	2
Number of biopsies harvested from each donor:	5 (n = 3) to 6 (n = 9)	
Number of single cell isolated from each donor:	Median = 378′013 cells (ICR = 184′838–553′688 cells)	

ID: Identification number; ICR: Interquartile range; n: number of samples.

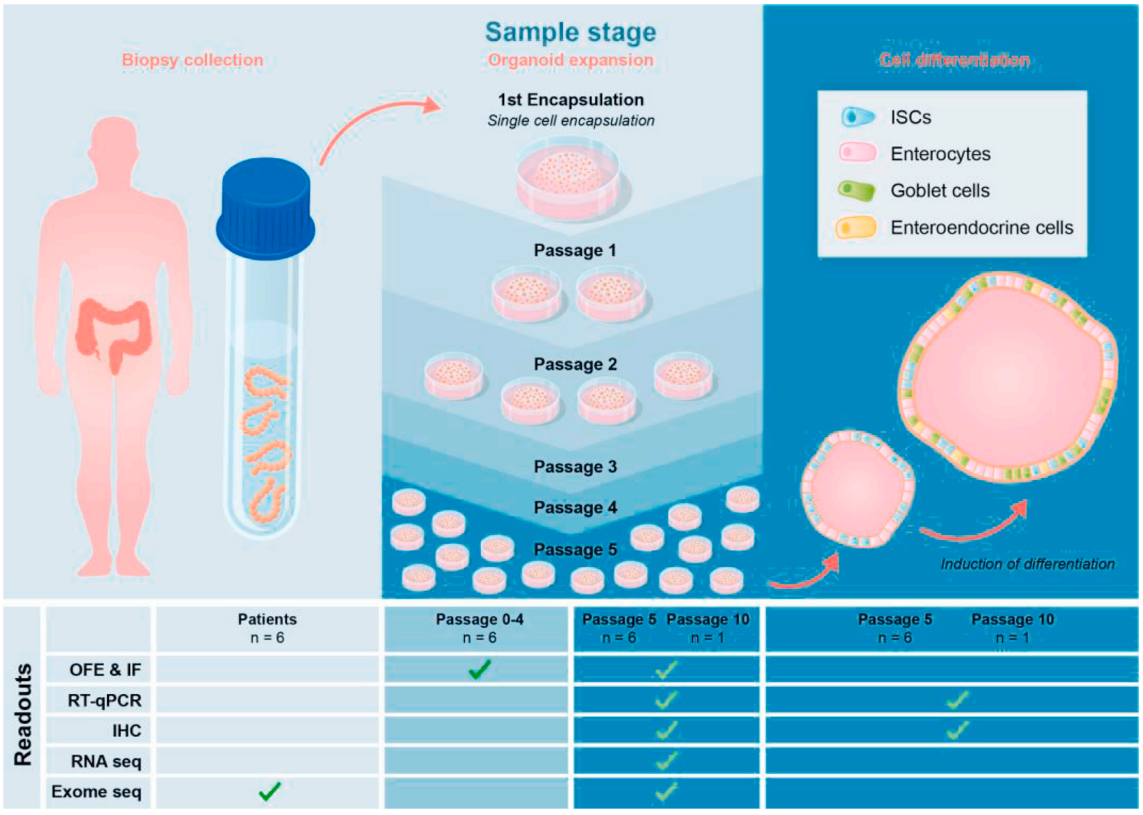

Fig. 1. Schematic illustration of the study design and readouts. Five to six colonic biopsies were collected endoscopically from six different patients (ID#6–11). One of the biopsies from each patient was used as a baseline sample for whole exome sequencing, whereas the remaining biopsies were used for organoid expansion. For all patients (n = 6), organoids were cultured in QGel CN99 or Matrigel for six passages (P0 – P5) albeit, cells from one patient sample were cultured for eleven passages (P0 – P10). The OFE and IF were determined at each passage, and at the sixth culture passage (P5) RT-qPCR, IHC, RNA- and exome sequencing were performed. Following induction of intestinal stem cell (ISC) differentiation at P5, additional RT-qPCR and IHC were conducted.

supernatant was transferred to a new centrifuge tube coated with bovine serum albumin (0.1% in PBS) (BSA, Sigma-Aldrich). The tube was centrifuged at 300 *g* for 5 min at 4 °C, after which the supernatant was discarded. Crypt-derived single cells were attained by resuspending the crypt pellet in 3 ml of TrypLE Express (Thermo Fisher) supplemented with ROCK inhibitor. The tube was placed in a 37 °C water bath, and further mechanical dissociation was achieved using a P1000 pipette every 5 min. After a total duration of 20 min, the dissociation process was halted by adding ice-cold basal medium, and the tube was centrifuged three times at 500 *g* for 5 min at 4 °C. In between each centrifugation, half of the supernatant was removed and replaced with basal medium. After completion of the third centrifugation, the number of cells was manually quantified using a 0.0025 mm^2 Neubauer cell counting chamber (0.100 mm depth profounder). A final fourth wash was then performed using ice-cold basal medium, and after the last centrifugation (400 *g* for 5 min at 4 °C), cells were resuspended in a suitable volume of basal medium to obtain 2500 cells/μl (5x final concentration) and to be ready for encapsulation.

2.2. De novo establishment of organoid cultures from crypt-derived single cells

Colonic organoids were established by encapsulating crypt-derived single cells in both QGel CN99 (QGel SA, Lausanne, Switzerland), simply named hereafter as CN99, and Matrigel. Cell encapsulation in CN99 was performed according to the manufacturer instructions using QGel buffer A (2004A, QGel SA) diluted to a final concentration of 0.125 M with basal medium and supplemented with Jagged-1 (1.25 μM) (AnaSpec, Fremont, CA, USA) (buffer mix). Briefly, 80 μl of buffer mix was used to resuspend the CN99 lyophilized powder. After vortexing, 20 μl of cell suspension was added to the gel solution and carefully homogenized. Then, 20 μl domes were dispensed into a pre-warmed 48-well cell culture plate. The plate was placed in a 37 °C incubator and inverted every other minute until gelation occurred, thereby avoiding sedimentation of the cells (likewise done with Matrigel). Cell encapsulation in growth factor reduced Matrigel matrix (Corning Inc., Corning, NY, USA) was performed by mixing 50 μl Matrigel, 30 μl basal medium and 20 μl of cell suspension supplemented with Jagged-1. Subsequently, 20 μl domes (containing approximately 10′000 cells) of this mixture were allocated into culture wells of a pre-warmed 48-well cell suspension culture plate (CELLSTAR, Greiner Bio-One, Kremsmünster, Austria). After a total duration of 20 min in the 37 °C incubator, 330 μl of culture medium was added on top of the domes. Plates were then incubated at 37 °C and 5% CO_2. The culture medium was replaced every 2–3 days throughout all experiments and ROCK inhibitor was maintained in the culture media for the first days of culture. To optimize growth conditions and improve the *de novo* organoid forming efficiency (OFE) at P0 in CN99, variations of the standard culture medium were tested on crypt-derived freshly isolated single cells from three patients (ID#3–5). These included removal of both SB202190 and N-acetylcysteine (NAC), or each of them separately (removal of SB202190 and NAC have been previously reported to have beneficial effects on growth and survival of prostate organoids [24]), and results were benchmarked against IntestiCult Organoid Growth Medium (Human) (STEMCELL Technologies Inc., Vancouver, BC, Canada) (both in CN99 and Matrigel). After the optimization, the commercially available IntestiCult was chosen for the validation study (ID# 6–12). All established organoid cultures were tested negative for mycoplasma contamination using MycoAlert Mycoplasma detection kit (Lonza, Basel, Switzerland).

2.3. Passaging of organoids

Passaging was performed at an interval of 8–11 days by adding 300 μl TrypLE Express (supplemented with ROCK inhibitor, 10 μM) to each well and mechanically disrupting the domes using a P1000 pipette. After up to 3 min incubation, dissociated gels were transferred to a 15 ml centrifuge tube pre-coated with BSA (0.1%). An additional 500 μl of TrypLE Express was used to rinse all wells of the same culture condition. The tube was then placed in a 37 °C water bath, and organoids were further dissociated into single cells every 5 min using a P1000 pipette or a 1 ml syringe (Becton Dickinson, Franklin lakes, NJ, USA) with a 23G cannula (KD Medical GmbH, Berlin, Germany). The status of organoid dissociation into single cells was regularly checked by observing the sample under a microscope. When satisfactory single cell suspension had been attained, TrypLE was quenched through dilution with ice-cold basal medium. The tube was washed and centrifuged at 300 *g* for 5 min at 4 °C three times, after which the number of cells was quantified, and cells were re-seeded in CN99 or Matrigel, at a cell density of approximately 10′000 cells per well (i.e., 20 μl dome). For handling reasons, only a portion of the cells (400′000–800′000 cells) were re-seeded at each passage. For six patient samples (ID#6–11), organoids were cultured for six passages (P0 – P5), albeit for one randomly selected patient sample (ID#8), the culture duration was extended for up to eleven passages (P0 – P10).

Following passaging at completion of P4 (ID#7) and P3 (ID#10) single cells (median 88′000 cells, ICR: 70′250–112′500 cells) were cryopreserved in Recovery Cell Culture Freezing Medium (Thermo Fischer Scientific) at – 80 °C for approximately four weeks before being thawed and re-seeded in accordance with the standard protocol described above.

2.4. Organoid forming efficiency (OFE), cell incremental factor (IF) and projected total number of cells

OFE: For preliminary experiments with organoids pre-established in Matrigel and during medium optimization for organoid establishment (ID#1–5), OFE was calculated on images taken respectively at day 4–5 (pre-established organoids) and day 8 (media optimization) using an ImageXpress Micro XL automated microscope (Molecular Devices, San Jose, CA, USA) with a 4x objective. Pictures were taken at multiple Z-positions and the resulting aligned and max-projected images were analyzed using MATLAB (Mathworks, Natick, MA, USA) software. OFE was calculated as the ratio between established organoids, and the total number of detected objects (single cells and organoids combined). For ID#6–11, during each culture passage, five representative images per well were taken at day 3–4 and again at day 7–8 using a Leica DMI3000 B inverted digital light microscope (Leica, Wetzlar, Germany) with a 5x objective. The number of organoids and single cells were semi-automatically quantified using an in-house MATLAB code based on a published adaptive threshold algorithm [25]. The automatic detection of objects by MATLAB was verified by the investigators, and objects not corresponding to cells or organoids (e.g., cell debris) were excluded from the analysis.

IF: The cell IF was defined as the ratio between the number of cells collected at the end of each passage and the number of cells seeded at the beginning of that passage.

Projected total number of cells: The projected total number of cells corresponds to the number of cells that would have been obtained if all cells had been kept in culture from P0 – P5. For each cell passage this was calculated by multiplying the number of cells seeded by each sequential IF per passage.

2.5. Organoid differentiation, RT-qPCR and immunohistochemistry (IHC)

Organoid differentiation: At the end of the sixth culture passage (P5, day 7) in IntestiCult medium, a portion of the organoids was collected for RNA extraction and immunohistochemistry (IHC), whereas the remaining portion was cultured for an additional 3–4 days in a differentiation medium (DM; standard culture medium (SCM) without Wnt3a, Rspo1, SB202190 and nicotinamide, Supplementary Table 1) [26,27] to induce cell differentiation before cells were harvested for subsequent analyses.

RT-qPCR: RNA was extracted by dissociating the organoids in TrypLE Express in accordance with the protocol described for single cell passaging. Cells were then centrifuged at 300 *g* for 5 min at 4 °C and washed with ice-cold DPBS. After centrifugation the pellet was resuspended in RP1 lysis buffer (Macherey-Nagel, Düren, Germany) and the tube was placed in - 20 °C, awaiting further processing and analysis. RNA extraction was achieved using a NucleoSpin TriPrep purification kit (Macherey-Nagel). Reverse transcription was performed using a Mastercycler (Eppendorf, Hamburg Germany) and RT-qPCR on a LightCycler 480 (Roche, Basel, Switzerland). All samples were run in three technical replicates. Analyzed genes included Leucine-rich repeat-containing G-protein coupled receptor 5 (*LGR5), Ki67,* Mucin 2 *(MUC2)*, Carbonic anhydrase II (*CAII)*, Cytokeratin 20 (*CK20)* and Chromogranin *A (CHGA)*. TATA-Box Binding Protein (*TBP*) was used to normalize gene expression data. The primer sequences are listed in Supplementary Table 2.

IHC: Organoids cultured in CN99 were harvested by directly transferring the domes to a biopsy cassette (Tissue-Tek Paraform cassettes, Sakura Finetek Europe, Alphen aan den Rijn, The Netherlands) using a spatula, after which they were fixed with paraformaldehyde and subsequently embedded in paraffin (Tissue-Tek Paraform Processing/Embedding Medium Formula 3, Sakura Finetek Europe) using an automated Tissue-Tek VIP vacuum infiltration processor (Sakura Finetek Europe). Organoids cultured in Matrigel were transferred to a 50 ml Falcon tube (Becton Dickinson) by adding cold DPBS and mechanically disrupting the Matrigel domes with a pipette. After centrifugation, organoids were embedded into an artificial clot achieved by resuspending the organoids in human plasma (isolated in house) and adding bovine thrombin (Merck, Darmstadt, Germany). Cells were then fixed with paraformaldehyde (4%) (Sigma-Aldrich) and embedded in paraffin. Slides were stained with hematoxylin eosin (H&E, Merck) before microscopic evaluation. Selected representative slides were then stained with periodic acid-Schiff (PAS, VWR, Radnor, PA, USA) along with antibodies against MUC2 (FLEX mouse anti-human MUC2, clone CCP58, ready-to-use, DAKO, Agilent Technologies, Santa Clara, CA, USA), CK20 (FLEX monoclonal mouse anti-human cytokeratin 20, clone K 20.8, ready-to-use, DAKO, Agilent Technologies), CHGA (mouse monoclonal anti-human chromogranin A LK2H10, ready-to-use, Ventana, Roche) and Ki67 (FLEX monoclonal mouse anti-human Ki67, clone MIB-1, ready-to-use, DAKO, Agilent Technologies).

H&E and PAS stains were performed using a Tissue-Tek Prisma Plus automated slide stainer (Sakura Finetek), whereas antibody stains were performed using a Ventana Benchmark ULTRA (Roche) or Dako Omnis (Agilent Technologies) automated solutions. Slides of human appendix (CK20, MUC2 and CHGA) or human tonsils (Ki67) were used as positive antibody controls and were stained simultaneously with the respective study samples.

2.6. RNA sequencing

Organoids were harvested for RNA extraction (n = 6 in each group) at the end of the sixth culture passage (P5, day 7) as described above. Quantification and purity were assessed using a NanoDrop spectrophotometer (Thermo Fisher, A260/A280 and A260/230 of approximately 2), whereas RNA quality was assessed using a Bioanalyzer automated electrophoresis (Agilent Technologies, RIN > 9). RNA sequencing (RNA-seq) (Illumina PE150 system, Illumina, San Diego, CA, USA) was performed by Novogene Ltd. (Beijing, China), and bioinformatic analyzes were subsequently conducted at the Biotech Research and Innovation Center (BRIC, University of Copenhagen, Denmark). The raw reads were quality assessed with FastQC [28] and FastQ Screen [29] and afterwards trimmed using Trimmomatic (v.0.32) [30]. The trimmed reads were aligned to the hg38 genome assembly using STAR (v.2.5.1a) [31] in two-pass mode and guided by a RefSeq (UCSC, 2018.08.05) gene annotation.

After mapping, reads were assigned to genes using featureCounts (v.1.5.1) [32] thereby generating a count table. In R software (v.3.5.1) [33] the DESeq2 (v.1.22.1) [34] package was used for statistical analysis of the count data.

Using the clusterProfiler package (v.3.10.1) [35] Gene Set Enrichment Analysis (GSEA, Broad Institute Inc., Cambridge, MA, USA) [36,37] was run against the Molecular Signature Database (MsigDB, Broad Institute Inc.) [37,38] focusing on the hallmark gene set collection.

Raw transcriptomic paired-end data sets GSE104178 [39] and GSE50760 [40], containing RNA seq data from healthy human colonic epithelium, primary colorectal cancer (CRC) and metastases, were downloaded from Gene Expression Omnibus (GEO) [41,42]. To make these public data comparable to our own, we first trimmed the reads with Trim Galore (v.0.4.4) [43] and then processed the data identically to our own data. After combining the gene counts of the three datasets in R and normalizing for sequencing depth with the EDASeq package (v.2.6.2) [44] we removed visible batch effect (estimated from principal component analysis (PCA) plots) with the RUVg function from the RUVSeq package (v.1.6.2) [45].

2.7. Whole exome sequencing

Immediately after harvesting (before initial cell isolation), one biopsy per donor was snap frozen in liquid nitrogen and stored at - 80 °C until processing (n = 6). The biopsies were mechanically dissociated using a TissueLyser (Qiagen, Venlo, The Netherlands), after which DNA was extracted with the NucleoSpin TriPrep purification kit.

After the organoids had been cultured for a total duration of six passages (P5) DNA was collected and extracted (n = 6 in each group). Furthermore, two additional samples (one cultured in CN99 and one in Matrigel) were extracted at the end of the eleventh culture passage (P10, 107 days in culture). DNA concentrations were determined using a NanoDrop spectrophotometer and Qubit fluorometer (Thermo Fisher). With the purpose of comparing sequencing reads from cells cultured *in vitro* to the baseline reads from the snap-frozen biopsies, whole exome sequencing was performed using NextSeq500 or NovaSeq6000 platforms (Illumina). This was done at the Center for Genomic Medicine (Rigshospitalet, The Kennedy Center, Glostrup, Denmark) in accordance with published protocols [46]. In brief, 200 ng of DNA was used to prepare sequencing libraries and fragmentation (approximately 300 base pair fragments) was done using a Covaris S2 sonicator (Covaris Inc., Woburn, MA, USA). A KAPA HTP Library Preparation kit (Roche) was used for adaptor ligation. A SureSelectXT Clinical Research Exome kit (Agilent) was utilized for exome enrichment, after which paired-end sequencing was conducted. BWA-MEM (v.0.7.12) [47] was used to trim and map reads to hg19/GRCh37 reference genome. The Genome Analysis Toolkit (GATK, v.3.8.0, Broad Institute Inc.) [48] was applied to pre-process alignment files, and GATK (v.3.8.0) MuTect2 was used to subsequently analyze the alignment files, and called variant were filtered with Ingenuity Variant Analysis (v.5.5) (Qiagen).

2.8. Statistics

Statistical analyzes of experimental data were performed using GraphPad Prism 8.0.0 (GraphPad Software, San Diego, CA, USA). The cell expansion, IF, OFE and the gene expression data were analyzed using non-parametric Wilcoxon matched pairs signed rank test, and the attained results were considered statistically significant at $p < 0.05$. Bioinformatic analysis of RNA- and whole exome sequencing is described in sections of relevance above.

2.9. Regulatory approvals

The project was approved by the Danish Data Protection Agency as well as by the Scientific Ethics Committee of the Copenhagen Capital Region. All patients received written and oral information before giving their written consent.

3. Results

3.1. De novo establishment and expansion of colonic organoids using fully defined hydrogels

The implementation of a fully defined ECM for the establishment and expansion of intestinal organoids with cells obtained directly from fresh biopsies, constitutes a key step towards translational applications.

QGel CN99 is a mechanically dynamic polyethylene glycol (PEG)-based hydrogel with an initial shear modulus (G') of 450 Pa, which ends in the same range as that of Matrigel (10–50 Pa, depending on the concentration) after 7–10 days of cell culture. This hydrolytic softening facilitates harvesting of cells during organoid passaging. The novel CN99 gel was identified based on previously published gel screening methods [49] and on works describing the growth of intestinal organoids in defined hydrogels [16–18]. For simplified handling CN99 employs a cross-linking chemistry for hydrogel formation, namely Michael-type conjugate addition [17,50], that does not rely on enzymes (e.g., FXIII) [16,18]. Furthermore, in contrast to previously described hydrogels that require mixing of several components before use, all CN99 precursors are lyophilized in a single ready-to-use vial allowing hydrogel formation and cell encapsulation by simply adding buffer and cells to the vial.

CN99 was initially tested using organoids pre-established and expanded in Matrigel for several passages (ID#1–3) in SCM (Supplementary Table 1) [27]. Cells grown in CN99 showed similar organoid forming efficiency (OFE) and morphology compared to the BME-benchmark, Matrigel (Supplementary Fig. 1). Based on the promising results, CN99 was selected for further investigation and biological validation for the establishment and expansion of human colonic organoids directly from cells harvested from fresh endoscopically obtained colon biopsies, with the goal of completely bypassing the use of BME.

Of note, for the first *ex vivo* culture passage (P0), freshly isolated single cells were encapsulated, instead of crypt fragments, to allow for better control of the starting cell seeding density and to guarantee a precise comparison of organoid formation between CN99 and Matrigel. Cell seeding density was similarly controlled during the following passages allowing for the standardization of the entire cell expansion process.

To optimize the *ex vivo* establishment of organoids in CN99 at P0, we tested multiple variations of the SCM as well as the commercially available IntestiCult Organoid Growth Medium (Human). The OFE of

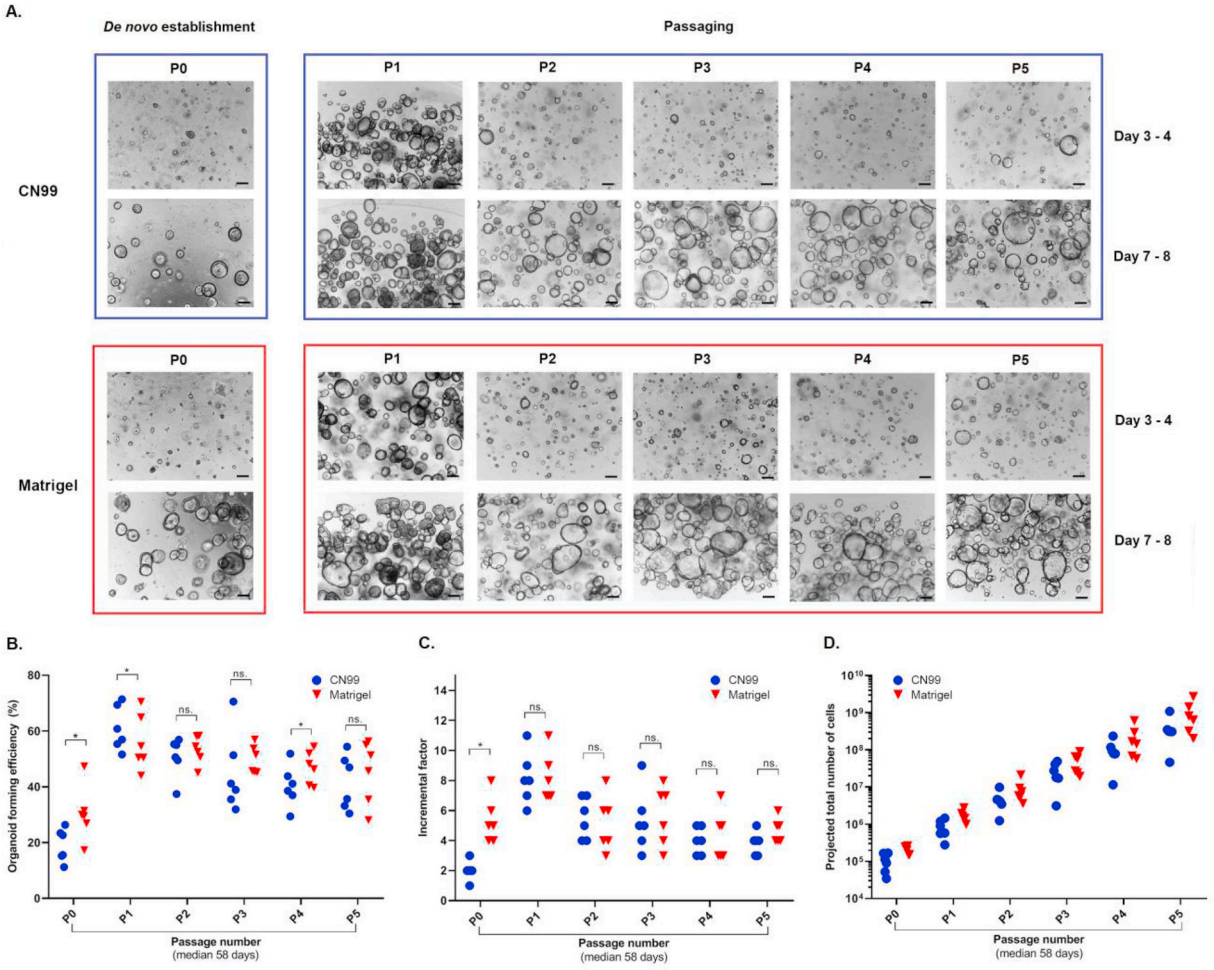

Fig. 2. Organoids cultured in QGel CN99 and Matrigel demonstrate comparable growth, cell expansion rate and organoid forming efficiency. A. Representative bright-field images (5x objective, ID#9) of organoids cultured in CN99 and Matrigel over time (day 3–4 to day 7–8, P0 – P5), scale bar = 100 μm. **B.** The organoid forming efficiency and **C.** incremental factor of cells (n = 6) cultured in CN99 (blue) or Matrigel (red). For each culture passage (P0 – P5) data were compared using Wilcoxon matched-pairs signed rank test. Comparisons were considered significant at $p < 0.05$ (*) and non-significant (ns.) comparisons are marked. **D.** Projections of the total number of cells, per initial biopsy, at the end of each passage, if all cells from the previous passage had been kept in culture. Results were calculated based on the starting number of cells seeded (per biopsy) at each passage and the respective incremental factor for that passage. (For interpretation of the references to color in this figure legend, the reader is referred to the Web version of this article.)

cells cultured in CN99 was comparable in all the tested conditions, albeit lower than in Matrigel (ID#3–5; Supplementary Fig. 2). Thus, to ensure reproducibility (e.g., minimize any variability related to SCM preparation), we decided to use the commercially available medium for all subsequent experiments.

Optimized culture conditions were subsequently applied to the encapsulation of freshly isolated crypt-derived single cells from six different patient biopsies (ID#6–11). For all biopsies, organoids were cultured for six passages (P0 to P5) (median = 58 days, ICR = 56–59), whereas cells from one randomly selected patient ID (ID#8) were cultured for up to eleven passages (P0 to P10, 107 days). Baseline information on cell donors, number of biopsies and the attained number of cells are summarized in Table 1.

Freshly isolated crypt-derived single cells cultured in CN99 and Matrigel formed organoids exhibiting the same spherical morphology, with rapid growth in both matrices (Fig. 2A).

The growth efficiency was assessed by determining the OFE and the cell incremental factor (IF) – both defined in the methods section. While the OFE (n = 6, Fig. 2B and Supplementary Fig. 3A) and the IF (n = 6, Fig. 2C and Supplementary Fig. 3B) at P0 were both significantly higher in Matrigel than in CN99 (p = 0.03), in the following passages they were overall comparable in the two matrices. The IF proved equivalent during all subsequent passages, whereas the OFE at P1 was higher in CN99 than in Matrigel and the opposite was observed at P4 (p = 0.03). The OFE and IF of the sample cultured up to P10 (n = 1) was retained within a similar range to that of the samples cultured from P1 to P5 (Supplementary Figs. 4A and B). The overall organoid growth in both ECMs is illustrated in Video S1 – S4.

Of note, single cells cryopreserved for approximately four weeks and subsequently re-seeded effectively formed new organoids in both CN99 and Matrigel.

To highlight the potential of *ex vivo* colonic organoid growth, we projected the total number of cells that would have been obtained per initial biopsy, if all cells from each passage were re-seeded (Fig. 2D). After six culture passages in CN99 we attained a median cell IF of 1210 (ICR: 728–3878) and 2896 in Matrigel (ICR: 1456–12,447), p = 0.03, with the difference exclusively due to the higher IF in Matrigel at P0. These data clearly demonstrate that colonic organoids were efficiently expanded *de novo* using the fully defined QGel matrix.

3.2. Organoids remain genetically stable, with transcriptomic profiles resembling normal epithelium

Organoid cultures were investigated for their *in vitro* genetic stability and RNA expression profiles.

Whole exome sequencing analyzes (average sequencing depth of 100x), comparing cells cultured in QGel CN99 and Matrigel (at P5: n = 6 in each group, at P10: n = 1 in each group) to the corresponding initial snap-frozen biopsies (n = 6), did not detect any acquired nucleotide substitutions. This is in line with previously published reports of genetic stability of intestinal organoids [27,51].

The PCA of the RNA sequencing (RNA-seq) data from individual

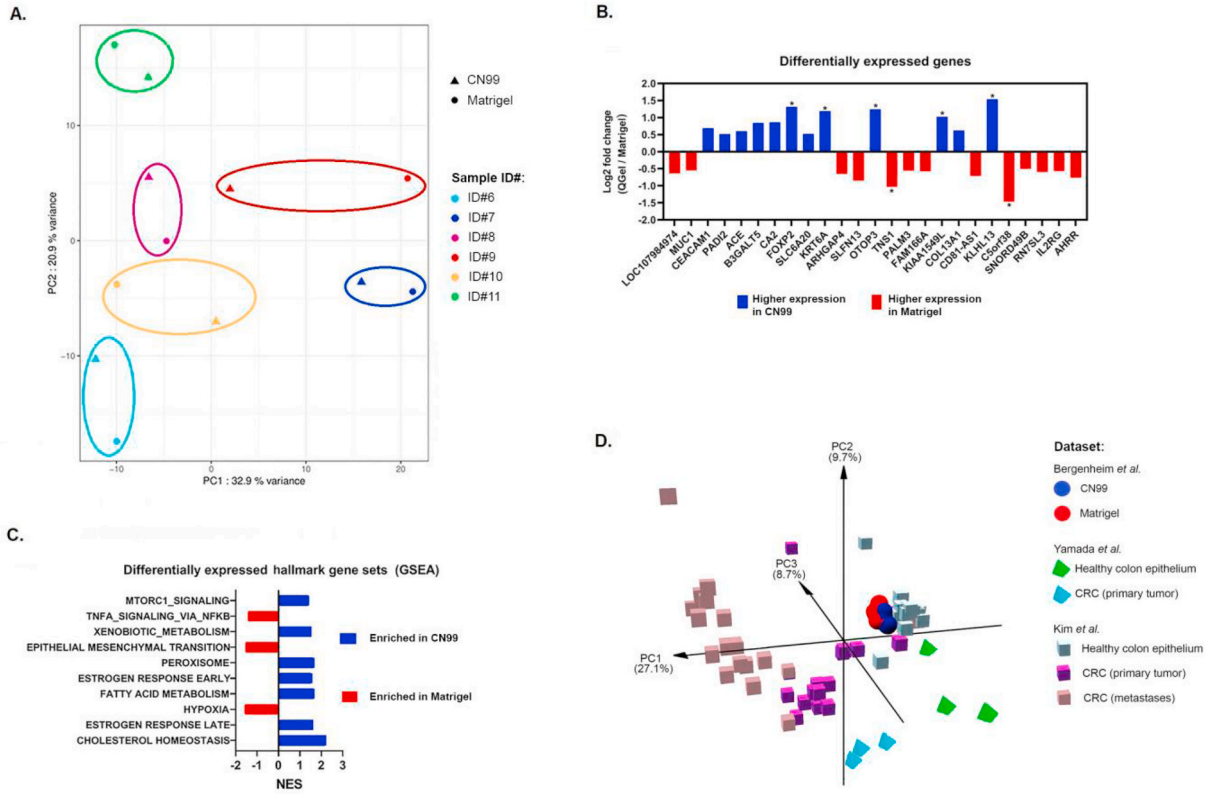

Fig. 3. Organoids cultured in QGel CN99 and Matrigel display comparable expression profiles resembling healthy colonic epithelium. A. Principal component analysis (PCA) plot of transcriptomic data from organoids cultured in CN99 (triangle) or Matrigel (circle) (ID#6–11). Data from each patient are represented with a different color. PC: principal component. **B.** Differential gene expression analysis of the two culture conditions (i.e., CN99 and Matrigel). Analyzes were conducted with a significance threshold of log2 fold change ≥ 0.5 combined with a false discovery rate (FDR) ≤ 10%, as well as using a stricter threshold (log2 fold change ≥ 1 and FDR ≤ 5%, marked with *). Abbreviations of differentially expressed genes are reported. Blue bars correspond to genes higher expressed in CN99 cultures and red bars correspond to genes with higher expression in Matrigel. **C.** The normalized enrichment score (NES) of differentially expressed hallmark gene sets (GSEA, FDR ≤ 5%) in cells cultured in CN99 (blue) and Matrigel (red). **D.** 3D PCA plot depicting transcriptomic data from cells cultured in CN99 or Matrigel (Bergenheim et al. GSE147133), as well as data from healthy tissue, primary colorectal cancer (CRC) and metastases from two independent datasets (Yamada et al. GSE104178 [39] and Kim et al. GSE50760 [40]) downloaded from the gene expression omnibus. (For interpretation of the references to color in this figure legend, the reader is referred to the Web version of this article.)

patient samples cultured for six passages in CN99 and Matrigel (n = 6 in each group) generally showed a tendency towards clustering of the individual patient samples, despite being cultured in different ECMs (Fig. 3A). In fact, expression profiles of all sample IDs, independent of ECM, displayed a Pearson's correlation coefficient ≥ 0.99, indicating a high degree of association. This was further supported by the fact that only 25 differentially expressed genes were detected between the two culture conditions, when using a threshold of log2 fold change ≥ 0.5 combined with a false discovery rate (FDR) ≤ 10% (Fig. 3B). However, when applying a stricter significance threshold (log2 fold change ≥ 1 combined with FDR ≤ 5%) to reduce the risk of inconsequential or false positive results, only seven differentially expressed genes were identified (marked by * in Fig. 3B). While the exact functions of some of these genes in the colonic epithelium remain obscure or even unknown (*KIAA1549L* and *C5orf38)*, other genes are known to be implicated in cell migration along with signal transduction to the cytoskeleton (*TNS1*), cell division (*KLH13*), as well as coding for proton-selective channels (*OTOP3*), cytoskeletal components (*KRT6A*) and transcription factors associated with intestinal development (*FOXP2*) (GeneCards – the human gene database, Weizmann Institute of Science, Rehovot, Israel and LifeMap Sciences, Alameda, CA, USA) [52].

The GSEA (FDR ≤ 5%) detected 10 well defined gene sets that were differentially expressed between cells cultured in CN99 and Matrigel (Fig. 3C). These represent definite signaling pathways and metabolic processes, and statistically significant differences were identified in the expression of genes regulated by nuclear factor kappa-light-chain-enhancer of activated B cells (NF-kB) in response to tumor necrosis factor alpha (TNF-α) (enriched in Matrigel), along with genes up-regulated through activation of the mammalian target of rapamycin complex 1 (mTORC1) (enriched in CN99), and those involved in epithelial-mesenchymal transition (EMT) and hypoxia (both enriched in Matrigel).

To investigate if, after *ex vivo* expansion in CN99 or Matrigel, the cultured cells did maintain expression profiles reminiscent of healthy primary tissue, we compared our RNA-seq data with two published datasets (GSE104178 and GSE50760) both containing healthy colonic epithelium CRC data. The PCA of our data combined with the published transcriptomic data revealed that both cells cultured in CN99 and Matrigel clustered notably closer to normal colonic epithelium, than to primary CRC or metastases (Fig. 3D), suggesting that they did not acquire a tumor-like expression profile. Importantly, although independently originated, data from healthy colonic epithelium from the two different published datasets clustered closely together, and the same was found for CRC samples, which demonstrates the validity of our data along with the analysis.

3.3. Colonic organoids retain the differentiation potential

Following expansion of colonic organoids in QGel CN99 and Matrigel, we demonstrated using RT-qPCR and IHC that the intestinal stem cells retained their multipotent differentiation capacity. Specifically, gene expression analysis of cells cultured for six passages showed that

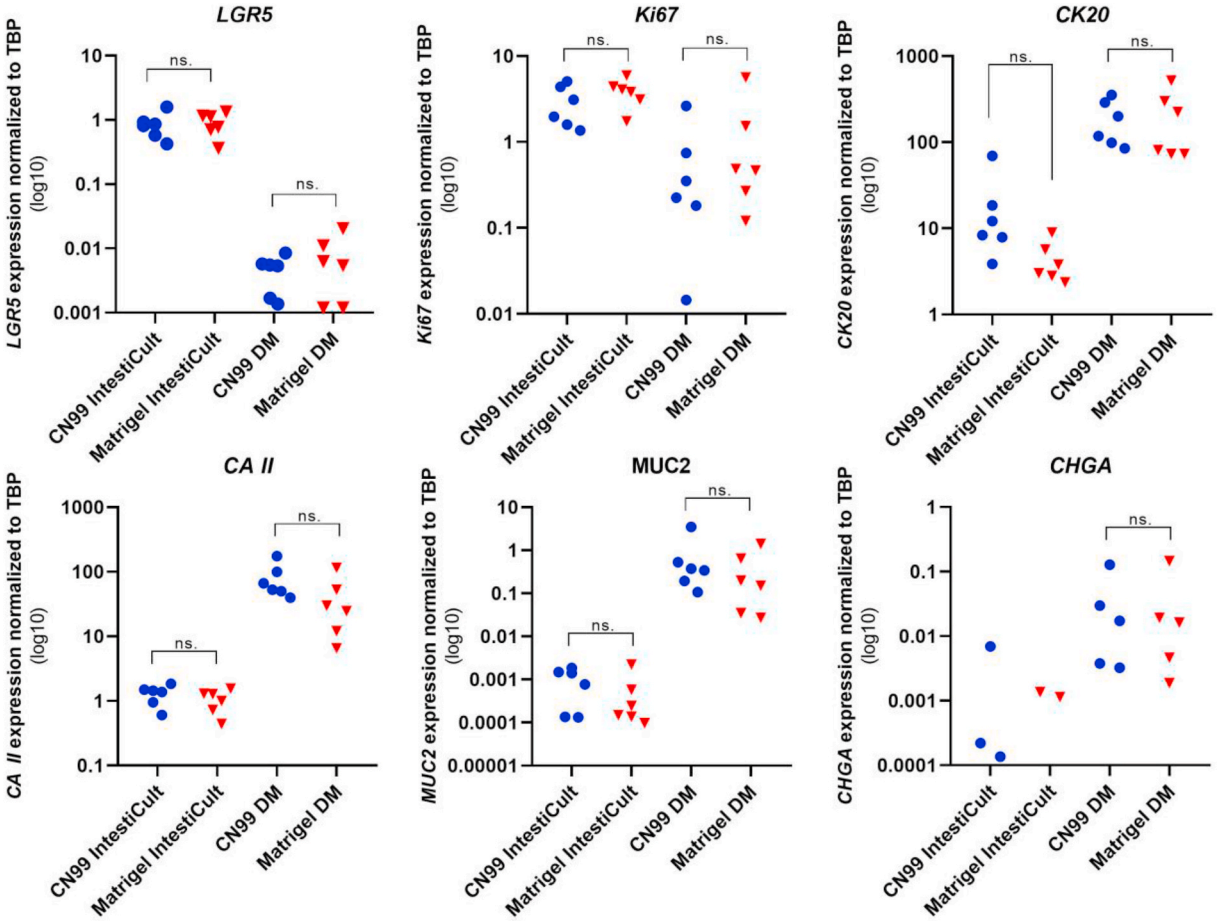

Fig. 4. Stemness and multilineage differentiation were maintained at comparable levels in QGel CN99 and Matrigel. RT-qPCR on organoids cultured in CN99 or Matrigel both before (cultured in IntestiCult medium) and after (cultured in differentiation medium, DM) induction of differentiation at P5. The expression levels of all target genes, Leucine-rich repeat-containing G-protein coupled receptor 5 (*LGR5*), *Ki67,* Mucin 2 *(MUC2*), Carbonic anhydrase II (*CAII*), Cytokeratin 20 (*CK20*) and Chromogranin *A (CHGA*), were compared (n = 6) using Wilcoxon matched pairs signed rank test and were considered significant at $p < 0.05$. Non-significant (ns.). TATA-Box Binding Protein (*TBP*) was used as an internal reference gene.

the stem cell marker *LGR5* was expressed at comparable levels in CN99 and Matrigel ($p = 0.69$, Fig. 4) in IntestiCult medium. Upon induction of differentiation by switching the culture medium from the commercially available medium to DM (Supplementary Table 1), the expression of *LGR5* was drastically reduced and no difference was detected between the two matrices ($p = 0.44$, Fig. 4). The expression of *Ki67* exhibited notable variations between different cell donors, most evidently prior to the induction of differentiation (Fig. 4), but no difference was detected between the two ECMs, before ($p = 0.09$) or after differentiation ($p = 0.84$). Low expression levels of differentiation markers *MUC2* (goblet cells), *CAII* (enterocytes), *CK20* (mature colonic epithelium) were maintained in both culture conditions before differentiation without any significant differences (*MUC2* $p = 0.56$, *CAII* $p = 0.44$ and *CK20* $p = 0.06$) and were equally inducible in both CN99 and Matrigel upon differentiation (*MUC2* $p = 0.31$, *CAII* $p = 0.22$ and *CK20* $p > 0.99$, Fig. 4). The levels of *CHGA* (enteroendocrine cells) proved undetectable in many samples and there was substantial variability between different cell donors. However, the expression was equally inducible in both culture conditions ($p = 0.81$, Fig. 4). Similar trends were observed in the sample cultured up to P10 ($n = 1$, Supplementary Fig. 4C).

The undifferentiated and differentiated cell states were confirmed with hematoxylin eosin (H&E) staining and by IHC (Fig. 5). In culture

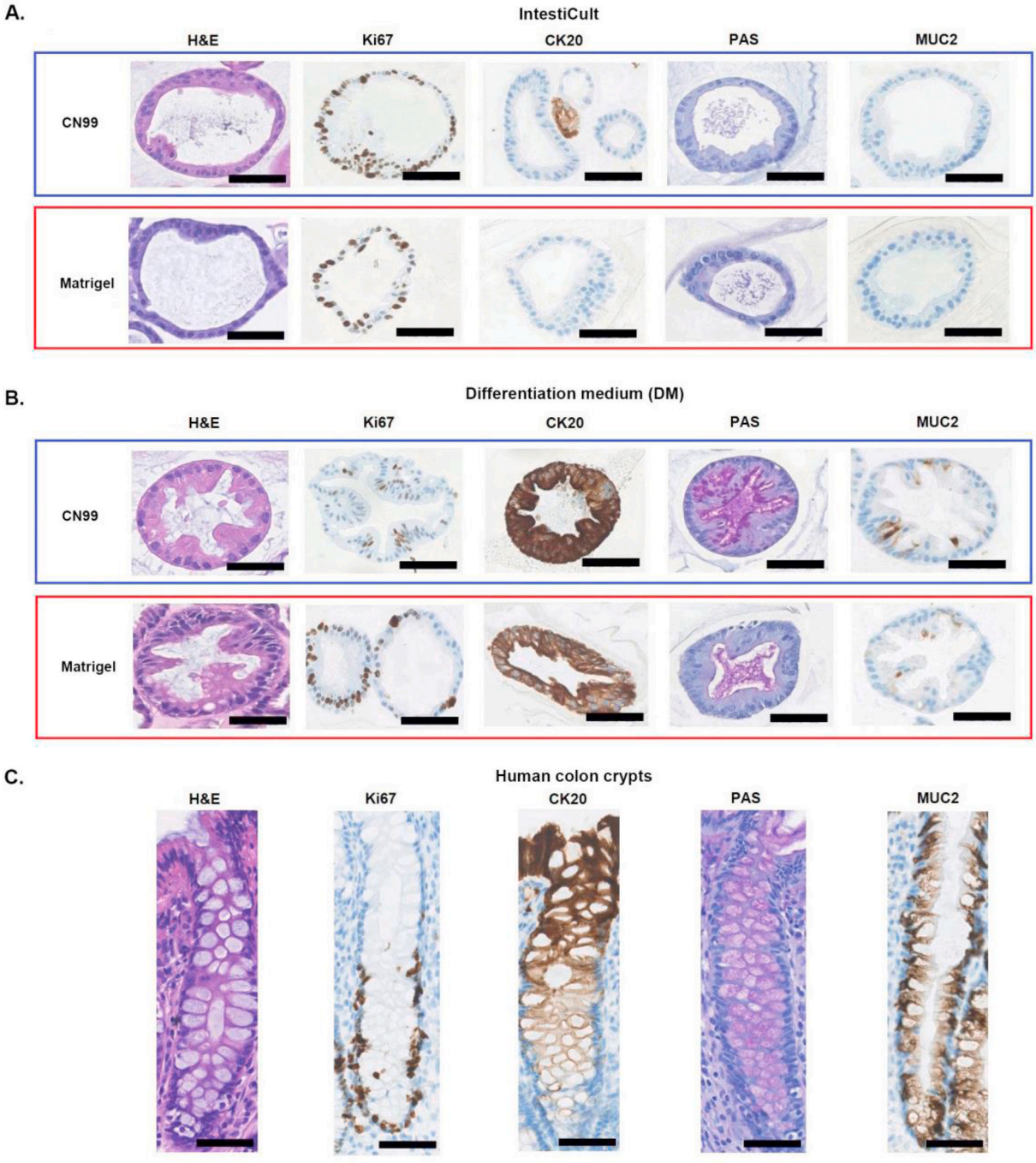

Fig. 5. Organoid morphology and IHC staining patterns were comparable in QGel CN99 and Matrigel. Representative images of human colon organoids **A.** before (cultured in IntestiCult medium) and **B.** after induction of differentiation (cultured in differentiation medium (DM)) stained with hematoxylin eosin (H&E), periodic acid-Schiff (PAS) and immunohistochemistry (IHC) for Ki67, MUC2 (Mucin 2) and CK20 (Cytokeratin 20). **C.** Longitudinal sections of human colon crypts stained with H&E, PAS or IHC (Ki67, MUC2 and CK20). Black scale bar = 50 μm.

conditions supporting the undifferentiated cell state (IntestiCult), cells cultured in both CN99 and Matrigel were mainly cubic, although some had a more abundant cytoplasm and cylindrical appearance. The nuclei were small, round or oval and, although heterogenous, the nuclei were generally basally aligned. Few cells had nucleoli and scattered mitoses could be identified. The glycocalyx layer was sparse. Focal positive reactions for CK20 were detected, and an estimated 80% of the cells expressed Ki67 (Fig. 5A). No goblet cells were observed, but some cells had PAS-positive mucin vacuoles in the cytoplasm (Fig. 5A). There were no positive reactions for MUC2 (Fig. 5A) or CHGA. Conversely, after cells had been allowed to differentiate for 3–4 days in DM, cells attained a more mature morphology. They became mainly cylindrical with small apical vesicles in the cytoplasm containing mucin. The nuclei were similarly small and round or oval, but predominantly basally located (Fig. 5B). The Ki67 index was estimated to be $< 10\%$, but with substantial variability between organoids (Fig. 5B). The glycocalyx layer became more affluent, and practically all cells stained strongly for CK20, but only a few cells stained positive for MUC2 (Fig. 5B). There were scattered goblet cells with dense hyperchromatic nuclei and a rich PAS-positive cytoplasm (Fig. 5B). The differences in MUC2 staining intensity *in vitro* and *in vivo* might indicate of changes in mucin composition. Scarcely any CHGA positive cells were detected, and importantly, no difference in the extent of cell differentiation was observed between organoids cultured in CN99 and Matrigel. Overall, cell morphology and staining properties of differentiated organoids were similar to the luminal part of healthy human colon crypts (Fig. 5C), although with some remaining Ki67-positive proliferative activity and notably less MUC2 positive reactions, whereas organoids cultured in IntestiCult overall bore closer resemblance to the crypts base. In general, using the fully defined QGel CN99, *ex vivo* expanded colon organoids demonstrated a differentiation capacity comparable to Matrigel.

4. Discussion

The primary focus of this study was to demonstrate that the fully defined hydrogel-based ECM QGel CN99 could reliably sustain *ex vivo* expansion of human colonic organoids, and possibly enable clinical translation (e.g., regenerative medicine). With this aim in mind, we investigated the following key process requirements: (i) bypass the use of BME, (ii) standardize the passaging process, (iii) achieve sufficient number of cells through expansion and passaging for either direct clinical use (e.g., autologous transplantation) or biobanking (generating HLA-matched master cell banks for allogenic transplantation), (iv) demonstrate the maintenance of the differentiation capacity of expanded cells, and (v) preliminarily explore the biosafety of *ex vivo* expanded cells, in relation to their genetic stability. We successfully achieved efficient *de novo* establishment, expansion and maintenance of human colonic organoids directly from patient biopsies, while sustaining genetic stability and differentiation capacity. Additionally, we were able to completely bypass the use of BME benchmark, thus overcoming its limitations that hamper translational applications of organoid technology. In this study, we did not investigate other natural or synthetic hydrogel systems as controls, as none so far have demonstrated superior growth efficiency to Matrigel [16–20].

To the best of our knowledge, we have demonstrated for the first time, the successful establishment of organoids directly from freshly harvested crypt-derived single cells using a fully defined hydrogel, with results comparable to the benchmark BME, Matrigel. Commonly, intestinal organoid cultures are established *de novo* in BME by encapsulating intestinal crypt fragments as opposed to single cells. In subsequent passages, the attained organoids are either mechanically or enzymatically dissociated into fragments or single cells allowing the number of organoids to increase exponentially. In our study, the direct use of single cells starting at P0, made it possible to consistently seed the same number of cells from multiple cell donors at every culture passage, which allowed for a rigorous and reliable comparison of the two culture conditions over time. In addition, we were able to cryopreserve single cells and subsequently re-establish organoid cultures after thawing. Of note, we successfully established organoids from both fresh biopsies as well as from biopsies kept on ice for 24 h before processing. Taken together, our data support the applicability of a fully defined hydrogel in combination with the single cell-based approach for efficient organoid expansion and biobanking. Consequently, our standardized method will help pave the way for clinical translation of the organoid technology.

An important criterion for the possible application of *ex vivo* expanded organoids in a clinical setting is the ability to obtain a sufficient quantity of cells in a reasonable timeframe. The projected total number of cells (Fig. 2D) demonstrates effective cell expansion in CN99, and except for the first culture passage (P0), the overall OFE and cell IF proved comparable to Matrigel. The cause of this observation at P0 remains unknown and may probably be multifactorial. On one hand we speculate that the difference might be due to the supportive effects of other cell types (e.g., differentiated epithelial cells, immune cells or mesenchymal cells) present in freshly harvested colonic biopsies [53] that temporarily remain viable in Matrigel (in contrast to in CN99) that support epithelial stem cell proliferation and/or survival. This hypothesis is in line with recent findings in mice, that $FOXL1^{+}$ mesenchymal cells contribute to the intestinal stem cell niche by production of Wnt proteins [54], a cell type likewise found in the human colon [55]. Likely, the supporting cells are not maintained in culture after P0, explaining the overall comparable results from P1 onwards. An alternative explanation could be that epithelial cells are able to cluster in Matrigel more so than in CN99, and that the locally increased cell density at P0 improves *de novo* organoid establishment. As shown in Supplementary Video 1–4, cell mobility is reduced in CN99, likely due to its higher initial stiffness as compared to Matrigel. Even if this aspect might impact organoid establishment at P0, we speculate that it did not play any major role, as in the following passages we did not observe differences in organoid growth between Matrigel and CN99. It is likely that following organoid formation at P0, the number of stem cells is enriched in both CN99 and Matrigel and, by seeding the same numbers of single cells, the supporting role of external factors (e.g., presence of other cell types or higher cell density) becomes dispensable after passaging. Nonetheless, further investigations are needed to explain this initial difference between CN99 and Matrigel.

We additionally investigated the ability of expanded cells to preserve their differentiation capacity. After *in vitro* induction, we clearly observed cell differentiation without any differences between the two matrices. Hence, despite prolonged culture in the fully defined QGel ECM, we maintained the multilineage differentiation capacity of the colonic stem cells, as supported by both the gene expression and IHC data. Nonetheless, the cytologic evaluation of H&E stained cells in combination with the limited MUC2 staining and the minimal CHGA positive reactions indicate that secretory lineage cell differentiation is only partially achieved in both ECM when simply omitting important niche factors (i.e., Wnt3a, Rspo1, SB202190 and nicotinamide) from the culture medium. The applied differentiation model has apparent limitations in that organoid dissociation and cell apoptosis becomes evident already approximately 3–4 days after induction of differentiation, which impedes prolonged organoid maintenance. Preserving differentiated cells in human intestinal organoid cultures is a well-known and challenging phenomenon, but recently it was shown that by omitting a p38 inhibitor and adding insulin-like growth factor 1 (IGF-1) and fibroblast growth factor 2 (FGF-2) to the culture medium, differentiation towards the secretory lineage is improved, while simultaneously achieving stem cell- and organoid maintenance [56]. In our culture system with QGel CN99, the RT-qPCR data and IHC before induction of differentiation suggest that the stem cell population was effectively maintained in the IntestiCult medium at a comparable level to Matrigel. Furthermore, the transcriptome analysis clearly showed that the expression patterns of cells cultured in CN99 for six passages closely resembled healthy colonic epithelium. The differential gene expression analysis and GSEA did identify certain differences between cells cultured in CN99 and Matrigel,

especially in genes related to hypoxia (enriched in Matrigel) and metabolism (enriched in CN99). These observations could be attributed to differences in characteristics between CN99 and Matrigel (i.e., composition, initial stiffness and permeability). However, it remains to be determined whether the differences detected with GSEA translate into any biological differences as the overall transcriptome signatures were very similar. Also, with a limited number of samples the risk of false positive results needs to be taken into consideration as well.

Finally, the exome sequencing analysis together with the comparison of our transcriptomic data with two independent datasets, suggest that colonic organoids expanded in our culture conditions remain genetically stable, with transcriptomic profiles comparable to healthy colonic epithelium. While these data are highly promising, further *in vitro* and *in vivo* studies are needed to demonstrate complete cell biosafety for translation into the clinic.

In contrast to previously described defined matrices, CN99 can be easily used by any laboratory without specialized knowledge of hydrogel manufacturing. Since QGel matrices have a fully defined composition, they can be manufactured with high reproducibility and scalability, and in this way, they significantly contribute to the standardized use of organoids for clinical applications. Overall, we believe that the fully defined CN99 is a suitable alternative to the naturally derived BMEs (e.g., Matrigel) for colonic organoid establishment and growth. Finally, the combination with the commercially available IntestiCult culture medium further mitigates potential variability.

The use of intestinal organoids for regenerative applications will require that both the ECM and the culture medium are produced in accordance with regulatory guidelines. Hence, QGel SA is currently optimizing the hydrogel to comply with relevant regulatory requirements. We believe that the combined culture method employing the QGel CN99 matrix and IntestiCult medium presented in this paper builds the foundation for translational research of stem cell-based regenerative therapies for diseases characterized by barrier dysfunction, e.g., inflammatory bowel disease.

5. Conclusions

In conclusion, we have successfully identified an off-the-shelf and easy-to-use ECM that is fully defined and supports efficient establishment, expansion and biobanking of primary human colonic organoids. Furthermore, no pre-amplification in BME is required and as a result, we expect that QGel CN99 ECM will drastically improve standardization and reproducibility, while also enabling the use of organoids for clinical applications, such as regenerative and precision medicine.

Credit author statement

Conceptualization, F.B., G.F., J.T., J.B.S., O.H.N. and S.C.R.; Methodology, F.B., G.F., C.F.B., M.H. and J.T.; Investigation, F.B., G.F., C.F.B., M.H., L.B.R. and J.T.; Writing - original draft, F.B.; Writing - review & editing, F.B., G.F., C.F.B., L.B.R., M.H., J.T., J.B.S., S.C.R. and O.H.N. Supervision, J.B.S., O.H.N. and S.C.R; Funding acquisition, F.B., S.C.R. and O.H.N.

Funding information

The work performed at Herlev Hospital was supported by the Research Council of Herlev Hospital, Torben and Alice Frimodt's Foundation, Aage and Johanne Louis-Hansen Foundation [17-2B-0820], Aase and Ejnar Danielsen's Foundation [10–001972], Axel Muusfeldt's Foundation [2017–678], Dagmar Marshall's Foundation, Hartmann Foundation [A30985], Grosserer L.F. Foght's Foundation [21.283] along with The Foundation in Memory of Prosektor Axel Emil Søeborg Ohlsens and his Wife [6386 MT/IV].

Declaration of Competing interest

The authors declare the following financial interests/personal relationships which may be considered as potential competing interests:

F.B., J.B.S., L.B.R. and O.H.N. have no competing interests to declare.

G.F., M.H., C.F.B., J.T. and S.C.R. were employed by QGel SA at the time the research project was conducted.

Acknowledgements

We want to acknowledge Jens Vilstrup Johansen at BRIC as well as Christina Westmose Yde at The Center for Genomic Medicine for assisting with the bioinformatic analyzes of the RNA- and whole exome sequencing data.

Furthermore, we acknowledge Nicolas Chartier, Emanuele Gaudiello and Marc Sugnaux from QGel SA for their support in image analysis and for their assistance in performing certain cell experiments. We are, similarly, very grateful for the assistance of Fadime Pinar, Nine Scherling, Dorthe Gøth-Johansen and Eva Littrup Andersen at the research laboratory of the Dept. of Gastroenterology.

Appendix A. Supplementary data

Supplementary data to this article can be found online at https://doi.org/10.1016/j.biomaterials.2020.120248.

Data availability

The raw and processed data required to reproduce these findings are available from the corresponding author upon reasonable request. The QGel hydrogel (catalog number: CN99) is available on the QGel webshop at www.qgelbio.com/webshop/ or at info@qgelbio.com.

The RNA-seq data file generated during this study has been uploaded to GEO (GSE147133). Due to legal and ethical reasons patient-derived whole exome sequencing data cannot be shared.

References

[1] T. Sato, R.G. Vries, H.J. Snippert, M. van de Wetering, N. Barker, D.E. Stange, J. H. van Es, A. Abo, P. Kujala, P.J. Peters, H. Clevers, Single Lgr5 stem cells build crypt-villus structures in vitro without a mesenchymal niche, Nature 459 (7244) (2009) 262–265.

[2] M. Li, J.C. Izpisua Belmonte, Organoids - preclinical models of human disease, N. Engl. J. Med. 380 (6) (2019) 569–579.

[3] T. Nakamura, T. Sato, Advancing intestinal organoid technology toward regenerative medicine, Cell Mol Gastroenterol. Hepatol. 5 (1) (2018) 51–60.

[4] G. Berkers, M.P. van, A.M. Vonk, E. Kruisselbrink, J.F. Dekkers, K.M. de Winter-de Groot, H.G.M. Arets, R.E.P. Marck-van der Wilt, J.S. Dijkema, M. M. Vanderschuren, R.H.J. Houwen, H.G.M. Heijerman, E.A. van de Graaf, S. G. Elias, C.J. Majoor, G.H. Koppelman, J. Roukema, M. Bakker, H.M. Janssens, R. van der Meer, R.G.J. Vries, H.C. Clevers, H.R. de Jonge, J.M. Beekman, C.K. van der Ent, Rectal organoids enable personalized treatment of cystic fibrosis, Cell Rep. 26 (7) (2019) 1701–1708.

[5] M. van de Wetering, H.E. Francies, J.M. Francis, G. Bounova, F. Iorio, A. Pronk, H. W. van, G.J. Van, A. Taylor-Weiner, L. Kester, A. McLaren-Douglas, J. Blokker, S. Jaksani, S. Bartfeld, R. Volckman, S.P. van, V.S. Li, S. Seepo, P.C. Sekhar, K. Cibulskis, S.L. Carter, A. McKenna, M.S. Lawrence, L. Lichtenstein, C. Stewart, J. Koster, R. Versteeg, O.A. van, J. Saez-Rodriguez, R.G. Vries, G. Getz, L. Wessels, M.R. Stratton, U. McDermott, M. Meyerson, M.J. Garnett, H. Clevers, Prospective derivation of a living organoid biobank of colorectal cancer patients, Cell 161 (4) (2015) 933–945.

[6] R.P. Fordham, S. Yui, N.R. Hannan, C. Soendergaard, A. Madgwick, P.J. Schweiger, O.H. Nielsen, L. Vallier, R.A. Pedersen, T. Nakamura, M. Watanabe, K.B. Jensen, Transplantation of expanded fetal intestinal progenitors contributes to colon regeneration after injury, Cell Stem Cell 13 (6) (2013) 734–744.

[7] S. Sugimoto, Y. Ohta, M. Fujii, M. Matano, M. Shimokawa, K. Nanki, S. Date, S. Nishikori, Y. Nakazato, T. Nakamura, T. Kanai, T. Sato, Reconstruction of the human colon epithelium in vivo, Cell Stem Cell 22 (2) (2018) 171–176.

[8] S. Yui, T. Nakamura, T. Sato, Y. Nemoto, T. Mizutani, X. Zheng, S. Ichinose, T. Nagaishi, R. Okamoto, K. Tsuchiya, H. Clevers, M. Watanabe, Functional engraftment of colon epithelium expanded in vitro from a single adult Lgr5(+) stem cell, Nat. Med. 18 (4) (2012) 618–623.

[9] D. Dutta, I. Heo, H. Clevers, Disease modeling in stem cell-derived 3D organoid systems, Trends Mol. Med. 23 (5) (2017) 393–410.

[10] H. Miyoshi, K.L. VanDussen, N.P. Malvin, S.H. Ryu, Y. Wang, N.M. Sonnek, C. W. Lai, T.S. Stappenbeck, Prostaglandin E2 promotes intestinal repair through an adaptive cellular response of the epithelium, EMBO J. 36 (1) (2017) 5–24.

[11] C.M. Madl, S.C. Heilshorn, H.M. Blau, Bioengineering strategies to accelerate stem cell therapeutics, Nature 557 (7705) (2018) 335–342.

[12] C.S. Hughes, L.M. Postovit, G.A. Lajoie, Matrigel: a complex protein mixture required for optimal growth of cell culture, Proteomics 10 (9) (2010) 1886–1890.

[13] H. Tsuchiya, N. Sakata, G. Yoshimatsu, M. Fukase, T. Aoki, M. Ishida, Y. Katayose, S. Egawa, M. Unno, Extracellular matrix and growth factors improve the efficacy of intramuscular islet transplantation, PloS One 10 (10) (2015), e0140910.

[14] Z. Jabaji, G.J. Brinkley, H.A. Khalil, C.M. Sears, N.Y. Lei, M. Lewis, M. Stelzner, M. G. Martin, J.C. Dunn, Type I collagen as an extracellular matrix for the in vitro growth of human small intestinal epithelium, PloS One 9 (9) (2014), e107814.

[15] N. Sachs, Y. Tsukamoto, P. Kujala, P.J. Peters, H. Clevers, Intestinal epithelial organoids fuse to form self-organizing tubes in floating collagen gels, Development 144 (6) (2017) 1107–1112.

[16] N. Broguiere, L. Isenmann, C. Hirt, T. Ringel, S. Placzek, E. Cavalli, F. Ringnalda, L. Villiger, R. Zullig, R. Lehmann, G. Rogler, M.H. Heim, J. Schuler, M. Zenobi-Wong, G. Schwank, Growth of epithelial organoids in a defined hydrogel, Adv. Mater. 30 (43) (2018), e1801621.

[17] R. Cruz-Acuna, M. Quiros, A.E. Farkas, P.H. Dedhia, S. Huang, D. Siuda, V. Garcia-Hernandez, A.J. Miller, J.R. Spence, A. Nusrat, A.J. Garcia, Synthetic hydrogels for human intestinal organoid generation and colonic wound repair, Nat. Cell Biol. 19 (11) (2017) 1326–1335.

[18] N. Gjorevski, N. Sachs, A. Manfrin, S. Giger, M.E. Bragina, P. Ordonez-Moran, H. Clevers, M.P. Lutolf, Designer matrices for intestinal stem cell and organoid culture, Nature 539 (7630) (2016) 560–564.

[19] N. Gjorevski, M.P. Lutolf, Synthesis and characterization of well-defined hydrogel matrices and their application to intestinal stem cell and organoid culture, Nat. Protoc. 12 (11) (2017) 2263–2274.

[20] M.M. Capeling, M. Czerwinski, S. Huang, Y.H. Tsai, A. Wu, M.S. Nagy, B. Juliar, N. Sundaram, Y. Song, W.M. Han, S. Takayama, E. Alsberg, A.J. Garcia, M. Helmrath, A.J. Putnam, J.R. Spence, Nonadhesive alginate hydrogels support growth of pluripotent stem cell-derived intestinal organoids, Stem Cell Reports 12 (2) (2019) 381–394.

[21] S.R. Caliari, J.A. Burdick, A practical guide to hydrogels for cell culture, Nat. Methods 13 (5) (2016) 405–414.

[22] F.E. Holmberg, J.B. Seidelin, X. Yin, B.E. Mead, Z. Tong, Y. Li, J.M. Karp, O. H. Nielsen, Culturing human intestinal stem cells for regenerative applications in the treatment of inflammatory bowel disease, EMBO Mol. Med. 9 (5) (2017) 558–570.

[23] K.W. Schroeder, W.J. Tremaine, D.M. Ilstrup, Coated oral 5-aminosalicylic acid therapy for mildly to moderately active ulcerative colitis. A randomized study, N. Engl. J. Med. 317 (26) (1987) 1625–1629.

[24] M.L. Beshiri, C.M. Tice, C. Tran, H.M. Nguyen, A.G. Sowalsky, S. Agarwal, K. H. Jansson, Q. Yang, K.M. McGowen, J. Yin, A.N. Alilin, F.H. Karzai, W.L. Dahut, E. Corey, K. Kelly, A PDX/organoid biobank of advanced prostate cancers captures genomic and phenotypic heterogeneity for disease modeling and therapeutic screening, Clin. Canc. Res. 24 (17) (2018) 4332–4345.

[25] M.A. Borten, S.S. Bajikar, N. Sasaki, H. Clevers, K.A. Janes, Automated brightfield morphometry of 3D organoid populations by OrganoSeg, Sci. Rep. 8 (1) (2018) 5319.

[26] Y. Li, C. Soendergaard, F.H. Bergenheim, D.M. Aronoff, G. Milne, L.B. Riis, J. B. Seidelin, K.B. Jensen, O.H. Nielsen, COX-2-PGE2 signaling impairs intestinal epithelial regeneration and associates with TNF inhibitor responsiveness in ulcerative colitis, EBioMedicine 36 (2018) 497–507.

[27] T. Sato, D.E. Stange, M. Ferrante, R.G. Vries, J.H. van Es, S. Van den Brink, W. J. Van Houdt, A. Pronk, G.J. Van, P.D. Siersema, H. Clevers, Long-term expansion of epithelial organoids from human colon, adenoma, adenocarcinoma, and Barrett's epithelium, Gastroenterology 141 (5) (2011) 1762–1772.

[28] S. Andrews. FastQC: a quality control tool for high throughput sequence data. https://www.bioinformatics.babraham.ac.uk/projects/fastqc/Accessed 15 June 2020 .

[29] S. Andrews. FastQ Screen. http://www.bioinformatics.babraham.ac.uk/projects/fastq_screen/Accessed 15 June 2020 .

[30] A.M. Bolger, M. Lohse, B. Usadel, Trimmomatic: a flexible trimmer for Illumina sequence data, Bioinformatics 30 (15) (2014) 2114–2120.

[31] A. Dobin, C.A. Davis, F. Schlesinger, J. Drenkow, C. Zaleski, S. Jha, P. Batut, M. Chaisson, T.R. Gingeras, STAR: ultrafast universal RNA-seq aligner, Bioinformatics 29 (1) (2013) 15–21.

[32] Y. Liao, G.K. Smyth, W. Shi, featureCounts: an efficient general purpose program for assigning sequence reads to genomic features, Bioinformatics 30 (7) (2014) 923–930.

[33] R Core Team. R: A language and environment for statistical computing. R Foundation for Statistical Computing. https://www.r-project.org/Accessed 15 June 2020 .

[34] M.I. Love, W. Huber, S. Anders, Moderated estimation of fold change and dispersion for RNA-seq data with DESeq2, Genome Biol. 15 (12) (2014) 550.

[35] G. Yu, L.G. Wang, Y. Han, Q.Y. He, clusterProfiler: an R package for comparing biological themes among gene clusters, OMICS 16 (5) (2012) 284–287.

[36] V.K. Mootha, C.M. Lindgren, K.F. Eriksson, A. Subramanian, S. Sihag, J. Lehar, P. Puigserver, E. Carlsson, M. Ridderstrale, E. Laurila, N. Houstis, M.J. Daly, N. Patterson, J.P. Mesirov, T.R. Golub, P. Tamayo, B. Spiegelman, E.S. Lander, J. N. Hirschhorn, D. Altshuler, L.C. Groop, PGC-1alpha-responsive genes involved in oxidative phosphorylation are coordinately downregulated in human diabetes, Nat. Genet. 34 (3) (2003) 267–273.

[37] A. Subramanian, P. Tamayo, V.K. Mootha, S. Mukherjee, B.L. Ebert, M.A. Gillette, A. Paulovich, S.L. Pomeroy, T.R. Golub, E.S. Lander, J.P. Mesirov, Gene set enrichment analysis: a knowledge-based approach for interpreting genome-wide expression profiles, Proc. Natl. Acad. Sci. U. S. A 102 (43) (2005) 15545–15550.

[38] A. Liberzon, C. Birger, H. Thorvaldsdottir, M. Ghandi, J.P. Mesirov, P. Tamayo, The Molecular Signatures Database (MSigDB) hallmark gene set collection, Cell Syst 1 (6) (2015) 417–425.

[39] A. Yamada, P. Yu, W. Lin, Y. Okugawa, C.R. Boland, A. Goel, A RNA-Sequencing approach for the identification of novel long non-coding RNA biomarkers in colorectal cancer, Sci. Rep. 8 (1) (2018) 575.

[40] S.K. Kim, S.Y. Kim, J.H. Kim, S.A. Roh, D.H. Cho, Y.S. Kim, J.C. Kim, A nineteen gene-based risk score classifier predicts prognosis of colorectal cancer patients, Mol Oncol 8 (8) (2014) 1653–1666.

[41] R. Edgar, M. Domrachev, A.E. Lash, Gene Expression Omnibus: NCBI gene expression and hybridization array data repository, Nucleic Acids Res. 30 (1) (2002) 207–210.

[42] T. Barrett, S.E. Wilhite, P. Ledoux, C. Evangelista, I.F. Kim, M. Tomashevsky, K. A. Marshall, K.H. Phillippy, P.M. Sherman, M. Holko, A. Yefanov, H. Lee, N. Zhang, C.L. Robertson, N. Serova, S. Davis, A. Soboleva, NCBI GEO: archive for functional genomics data sets–update, Nucleic Acids Res. 41 (2013) D991–D995.

[43] F. Krueger. Trim Galore!: a wrapper tool around Cutadapt and FastQC to consistently apply quality and adapter trimming to FastQ files. http://www.bioinformatics.babraham.ac.uk/projects/trim_galore/Accessed 15 June 2020..

[44] D. Risso, K. Schwartz, G. Sherlock, S. Dudoit, GC-content normalization for RNA-Seq data, BMC Bioinf. 12 (2011) 480.

[45] D. Risso, J. Ngai, T.P. Speed, S. Dudoit, Normalization of RNA-seq data using factor analysis of control genes or samples, Nat. Biotechnol. 32 (9) (2014) 896–902.

[46] I.V. Tuxen, K.S. Rohrberg, O. Oestrup, L.B. Ahlborn, A.Y. Schmidt, I. Spanggaard, J. P. Hasselby, E. Santoni-Rugiu, C.W. Yde, M. Mau-Sorensen, F.C. Nielsen, U. Lassen, Copenhagen prospective personalized oncology (CoPPO)-Clinical utility of using molecular profiling to select patients to phase I trials, Clin. Canc. Res. 25 (4) (2019) 1239–1247.

[47] H. Li, Aligning sequence reads, clone sequences and assembly contigs with BWA-MEM, bioRxiv:arXiv:1303.3997 [q-bio.GN] (2013).

[48] A. McKenna, M. Hanna, E. Banks, A. Sivachenko, K. Cibulskis, A. Kernytsky, K. Garimella, D. Altshuler, S. Gabriel, M. Daly, M.A. DePristo, The Genome Analysis Toolkit: a MapReduce framework for analyzing next-generation DNA sequencing data, Genome Res. 20 (9) (2010) 1297–1303.

[49] A. Ranga, S. Gobaa, Y. Okawa, K. Mosiewicz, A. Negro, M.P. Lutolf, 3D niche microarrays for systems-level analyses of cell fate, Nat. Commun. 5 (2014) 4324.

[50] M.P. Lutolf, J.A. Hubbell, Synthesis and physicochemical characterization of end-linked poly(ethylene glycol)-co-peptide hydrogels formed by Michael-type addition, Biomacromolecules 4 (3) (2003) 713–722.

[51] X. Wang, Y. Yamamoto, L.H. Wilson, T. Zhang, B.E. Howitt, M.A. Farrow, F. Kern, G. Ning, Y. Hong, C.C. Khor, B. Chevalier, D. Bertrand, L. Wu, N. Nagarajan, F. A. Sylvester, J.S. Hyams, T. Devers, R. Bronson, D.B. Lacy, K.Y. Ho, C.P. Crum, F. McKeon, W. Xian, Cloning and variation of ground state intestinal stem cells, Nature 522 (7555) (2015) 173–178.

[52] G. Stelzer, N. Rosen, I. Plaschkes, S. Zimmerman, M. Twik, S. Fishilevich, T.I. Stein, R. Nudel, I. Lieder, Y. Mazor, S. Kaplan, D. Dahary, D. Warshawsky, Y. Guan-Golan, A. Kohn, N. Rappaport, M. Safran, D. Lancet, The GeneCards suite: from gene data mining to disease genome sequence analyses, Curr. Protoc. Bioinformatics. 54 (2016) 1.30.1–1.30.33.

[53] C.S. Smillie, M. Biton, J. Ordovas-Montanes, K.M. Sullivan, G. Burgin, D. B. Graham, R.H. Herbst, N. Rogel, M. Slyper, J. Waldman, M. Sud, E. Bolger, G. Velonias, A.L. Haber, K. Jagadeesh, S. Vickovic, J. Yao, C. Stevens, D. Dionne, L. T. Nguyen, A.C. Villani, M. Hofree, E.A. Creasey, H. Huang, O. Rozenblatt-Rosen, J. J. Garber, H. Khalili, A.N. Desch, M.J. Daly, A.N. Ananthakrishnan, A.K. Shalek, R. J. Xavier, A. Regev, Intra- and inter-cellular rewiring of the human colon during ulcerative colitis, Cell 178 (3) (2019) 714–730.

[54] M. Shoshkes-Carmel, Y.J. Wang, K.J. Wangensteen, B. Toth, A. Kondo, E. E. Massasa, S. Itzkovitz, K.H. Kaestner, Subepithelial telocytes are an important source of Wnts that supports intestinal crypts, Nature 557 (7704) (2018) 242–246.

[55] J. Kinchen, H.H. Chen, K. Parikh, A. Antanaviciute, M. Jagielowicz, D. Fawkner-Corbett, N. Ashley, L. Cubitt, E. Mellado-Gomez, M. Attar, E. Sharma, Q. Wills, R. Bowden, F.C. Richter, D. Ahern, K.D. Puri, J. Henault, F. Gervais, H. Koohy, A. Simmons, Structural remodeling of the human colonic mesenchyme in inflammatory bowel disease, Cell 175 (2) (2018) 372–386.

[56] M. Fujii, M. Matano, K. Toshimitsu, A. Takano, Y. Mikami, S. Nishikori, S. Sugimoto, T. Sato, Human intestinal organoids maintain self-renewal capacity and cellular diversity in niche-inspired culture condition, Cell Stem Cell 23 (6) (2018) 787–793.